He et al. Heritage Science (2024) 12:126
https://doi.org/10.1186/s40494-024-01245-x

Heritage Science

RESEARCH

Open Access

Exploring pottery origin by composition and technique comparison: a case study at the Daqu burial site, Beijing, China

Xiang He[1], Jingqi Wen[2*], Zhang He[3], InHee Go[1], Naitao Liu[4] and Hong Guo[1]

Abstract

Scientific analysis of excavated pottery reveals critical archaeological insights, yet data on Han Dynasty pottery remains limited. This study focuses on pottery artifacts excavated from the Daqu burial site in Beijing, renowned for their polychrome decorations and size. Utilizing optical microscopy (OM), X-ray diffraction (XRD), Fourier transform infrared spectroscopy (FT-IR), and X-ray Fluorescence (XRF), this study examined five substrate samples sourced from fragments of pottery towers and ellipse-shaped dishes. All samples exhibited similar inclusions and the same firing atmosphere. The mineralogical analysis indicated that quartz and feldspar are predominant components, with minor constituents like chlorite and kaolinite observed in the coarse pottery of the ellipse-shaped dish. Minor mineral variations suggest differences in firing temperatures. The resemblance between low-value pottery cups and delicate polychrome towers suggests they were crafted locally. These findings advance our understanding of ceramic materials and techniques in late Eastern Han Dynasty Beijing, providing crucial insights for future studies on ancient Chinese economy and society.

Keywords Han Dynasty pottery, Polychrome pottery towers, Mineralogical and geochemical analysis, Ancient Beijing archaeology

Introduction

The Han Dynasty (206 BC–220 AD) was a period of transformative change in China, profoundly impacting the funeral system among other aspects. The prevalence of Mingqi—crafted items specifically created for burial with the deceased—signified this cultural shift. Pottery towers, a common form of Mingqi, have been unearthed in numerous locations across China. However, the discovery of twenty polychrome pottery towers at the Daqu burial site in 2013 marked a unique occurrence, representing the first instance of finding such a large collection of polychrome towers outside the traditional center of the Han Dynasty, namely Shaanxi and Henan provinces [1, 2].

Situated 3 km southeast of Anding Town in the Daxing District of Beijing, as shown in Fig. 1, the Daqu burial site has unearthed a total of 32 tomb. Archaeological clues, including tomb architecture (brick tomb, Fig. 1) and burial products, dates 31 of these tombs to the Later Eastern Han period [2]. This is supported by thermoluminescence dating of pottery shards, suggesting a firing date of approximately B.P. 1875 ± 185 years. The excavated pottery towers, ranging from 33 to 72 cm in height, could be assembled into structures comprising two or three individual towers (Fig. 2). The pottery surface

*Correspondence:
Jingqi Wen
wjq101899@163.com
[1] Institute for Cultural Heritage and History of Science & Technology, University of Science and Technology Beijing, Beijing 100083, People's Republic of China
[2] National Centre for Archaeology, Beijing 100013, People's Republic of China
[3] Shaanxi Academy of Archaeology, Xi'an 710100, People's Republic of China
[4] Beijing Archaeology historic site museum, Beijing 100160, People's Republic of China

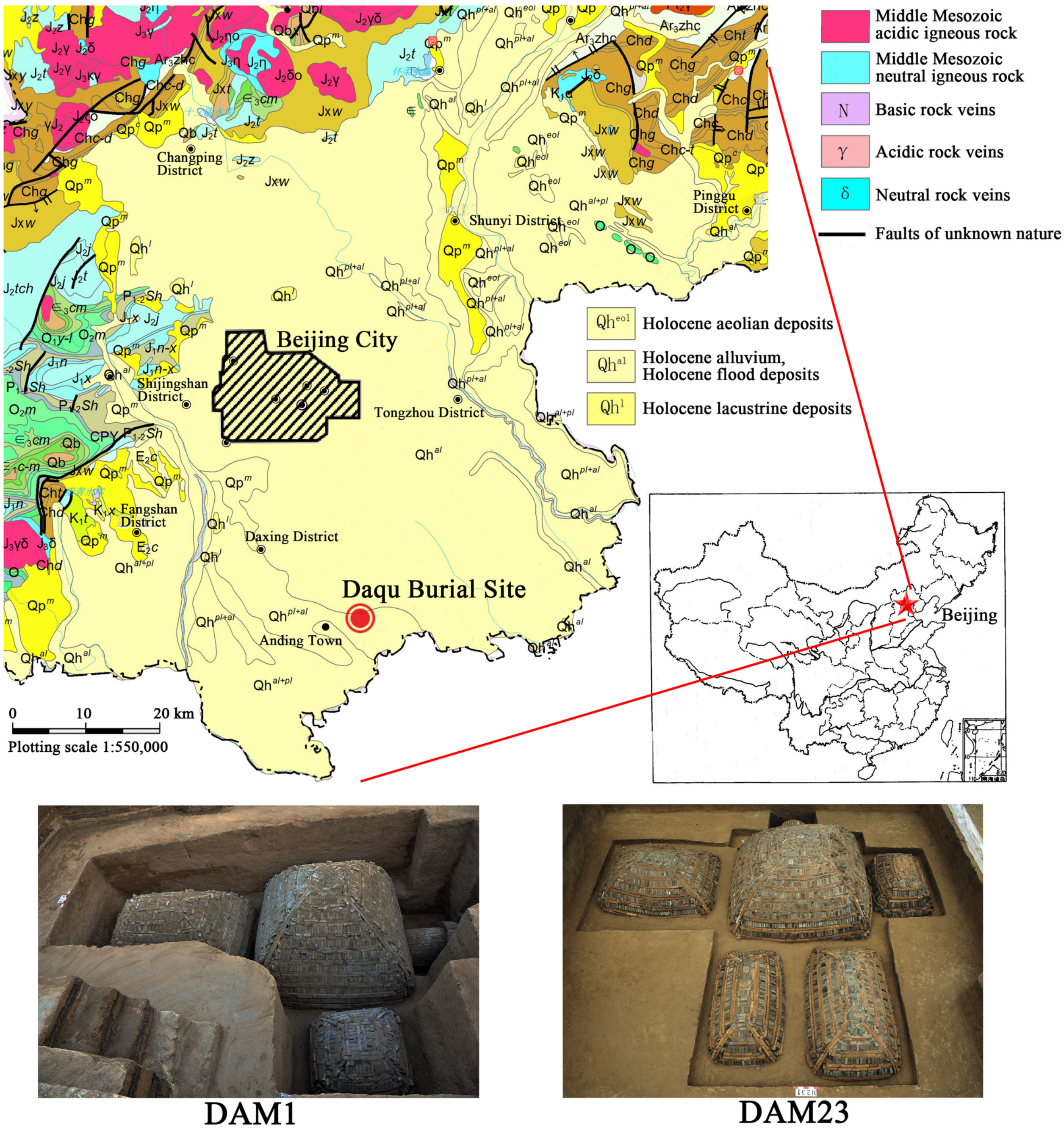

Fig. 1 Geological map of Beijing municipality, position of Daqu Burial site, and photographs of tombs

features painted beams, purlins, bracket systems, and animal heads, accompanied by abstract polychrome wall paintings utilizing black, white, and red pigments. These artifacts offer valuable insights into ancient construction methods and decorative arts, reflecting the Han Dynasty's beliefs in immortality.

Previous studies have explored typology and stylistic aspects of Han Dynasty pottery towers. The crafting of polychrome pottery towers with substantial volume and delicate aesthetics requires a high level of professional expertise. Consequently, the proprietors of these pottery towers have been identified as members of the middle and petty bourgeoisie [3–6]. In central China during the Han Dynasty, the building of exquisite pottery was a marker distinguishing the wealthy from ordinary people: "In the capital of the Han Dynasty, Chang'an city, a

Fig. 2 Examples of pottery towers and their archaeological numbers

pottery cooker was priced at two hundred coins. Acquiring a complete set of pottery Mingqi required a minimum of one thousand coins. This amount roughly equates to around 10 dan (石) [a unit of weight in ancient China, with a possible range of 13–30 kg] of rice, a cost beyond the means of ordinary people." [7].

Scientific analysis can provide a wealth of archaeological information to enhance the understanding to ancient society. Methods such as optical microscopy (OM), X-ray diffraction (XRD), Fourier transform infrared spectroscopy (FT-IR), and X-ray fluorescence (XRF) can unveil crucial information about raw materials, processing methods, firing atmosphere, firing temperature, and burial context. A comprehensive analysis can open avenues for discussing the origin, techniques, allocation, circulation, usage, mending, and abandonment of pottery, enabling a deeper exploration of technology levels, customs, organization, and inter-regional exchanges in ancient society [8–12]. However, scientific analysis of Han Dynasty pottery is currently limited [13, 14].

In this study, we conducted a detailed mineralogical and geochemical analysis of pottery samples from the Daqu burial site. The results provide insight into the materials and techniques employed in crafting pottery towers in the Beijing region during the late Eastern Han Dynasty, which will contribute to our understanding of ancient society.

Materials and methods

Sample selection

A variety of ceramics were excavated at the Daqu burial site, including bowls, cups, towers, bricks, and fragments. These potteries exhibit distinct textures. Notably, pottery towers exhibited a fine texture and relatively high strength, while ellipse-type dishes and certain pots displayed a rougher texture, with some parts showing surface disintegration. Five unrestorable shards, whose original positions could not be determined, were selected for analysis. They were from 4 different tombs. Based on their shape and the position at which they were unearthed, Samples 1 to 3 were traced to polychrome pottery towers, the origin of Sample 4 remained uncertain, and Sample 5 was identified as part of a coarse ellipse-shaped dish. Photographs and sample information are detailed in Fig. 3 and Table 1. These samples had previously undergone analysis using differential scanning calorimetry-thermal gravity analysis (DSC-TG), Fourier transform infrared spectroscopy, and dilatometry (DIL) [15].

Analytical procedures

Following ultrasonic washing and drying of the painted pottery fragments, the samples underwent slicing (approximately 30 μm thick) and double polishing for microscopic observation. Photographs of polished pottery samples are shown in Fig. 3. Additionally, 1.0 g of each sample was pulverized for subsequent XRD and XRF analyses.

L*a*b* values of the pottery cross sections were measured using a 3nh NH310 portable colorimeter (Guangdong Sanenshi Intelligent Technology Co., LTD, China).

A German Axioskop 40 was utilized for polarized and reflected light observations and photography of the pottery slices. Petrographic characteristics, mineral composition, and structural configuration of each sample were documented, and the contents of mineral components were estimated. A Keyence VHX-6000 microscope (Japan) facilitated the observation of the section structure of the pottery samples at magnifications ranging from 50× to 2000×.

Qualitative and semi-quantitative analysis of the composition of the pottery samples was conducted using a

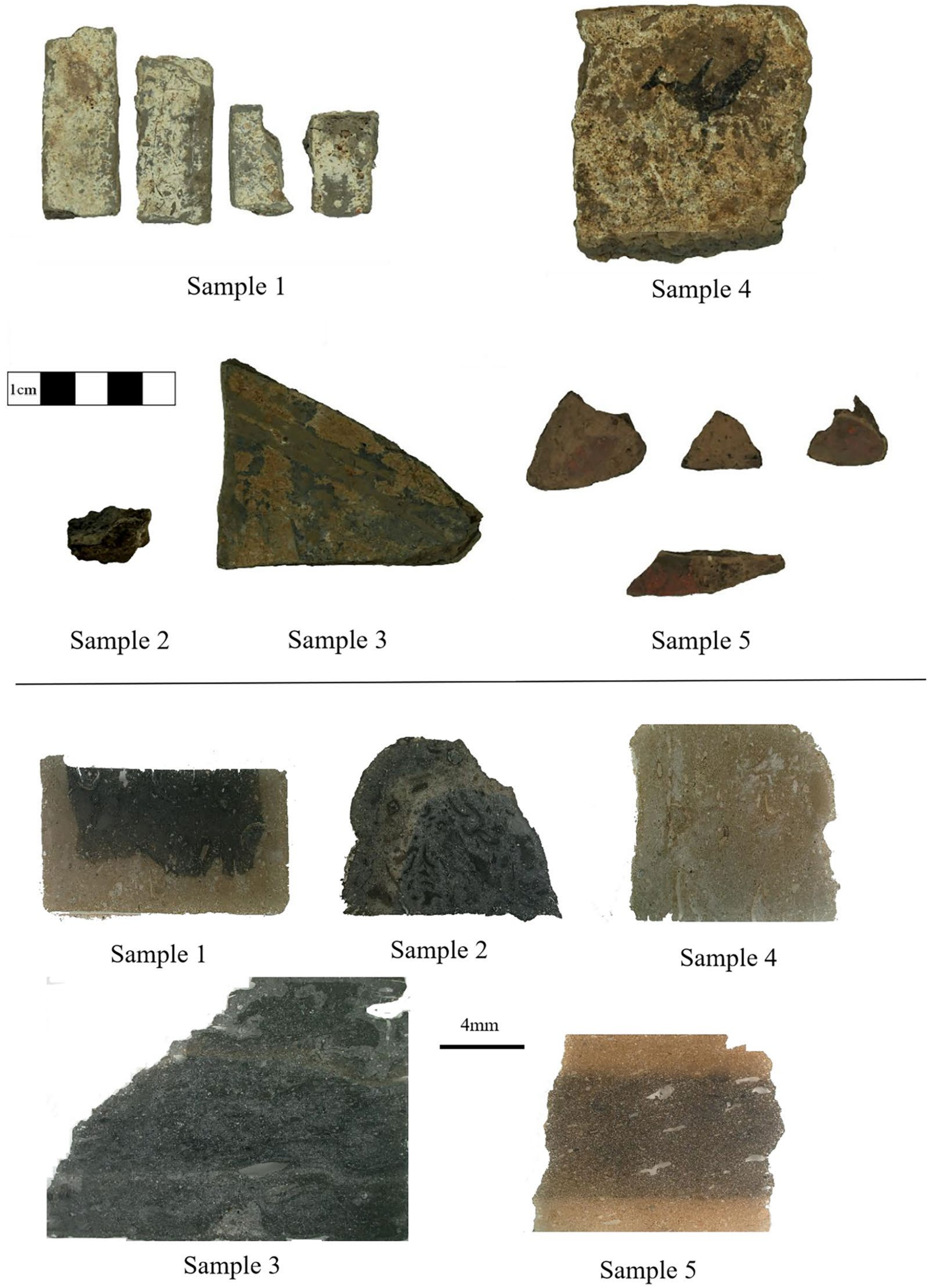

Fig. 3 Photographs of pottery samples chosen for analysis from the Daqu tomb and polished cross-section samples

D8 Advance X-ray diffractometer (Germany) equipped with a monochromized Cu radiation source. The 2θ scanning angle ranged from 3° to 70°.

For infrared analysis, the potassium bromide pellet method was employed, and Fourier transform infrared spectroscopy (FT-IR) was performed using a Nicolet Is 5 spectrometer (Thermo Fisher, United States). Spectra were recorded at a resolution of 2 cm^{-1}, with 64 scans added and averaged before Fourier transform. Spectra covering 400 cm^{-1} to 4000 cm^{-1} range

Table 1 Sample description

Sample No	Tomb Code	Sampling Position	Period	Quality	Chromatic Value			
					Cross section position	L*	a*	b*
Sample 1	DAM1	Window frame from a pottery tower	Eastern Han	Fine	Surface	58.57	1.29	10.77
					Core	40.29	0.05	3.62
Sample 2	DAM23	Fragment of pottery tower	Kingdom of Wei	Fine	Surface	47.45	0.38	3.78
					Core	40.54	0.24	3.94
Sample 3	DAM28	Alary part from pottery tower roof	Kingdom of Wei	Fine	Surface	43.15	1.63	7.58
					Core	48.58	0.54	4.04
Sample 4	DAM5	Fragment of unknow painted ceramic	Eastern Han	Fine	Surface	56.47	2.21	12.46
					Core	52.20	0.76	7.07
Sample 5	DAM28	Fragment from an ellipse-type dish	Kingdom of Wei	Coarse	Surface	51.22	10.52	21.41
					Core	41.73	5.75	13.14

L*:0/100: Black/White; a*:0/ – 60: Green; 0/ + 60: Red; b*:0/ – 60: Blues; 0/ + 60:Yellow

were previously published. [15] This study focused on absorption peaks occurring at a wave number lower than 1600 cm^{-1}.

An Idax EDAX Orbis X-ray Fluorescence Spectrometer (Ametek, the United States) was employed for qualitative and quantitative analysis of the chemical composition of the pottery samples, utilizing an Rh target X-ray tube operated at 40 kV and 500 μA. MBH 32XN7A was used as standard reference sample. Major oxides (SiO_2, Al_2O_3, K_2O, CaO, MgO, Fe_2O_3, TiO_2, MnO, and P_2O_5) were measured.

Results

Optical microscopy

Upon examination, all pottery samples demonstrated petrographic characteristics consistent with those of typical sedimentary loess found in northern China, predominated by quartz with less frequent feldspar and minimal inclusions (Fig. 4, Additional file 1: Fig. S1; Table 2). Samples 1–4 displayed no optical activity, while Sample 5 exhibited low optical activity.

The mineral compositions of Samples 1–3 were identical, while Sample 4 closely resembled them but lacked the presence of biotite. Calcite in the four samples was likely introduced as inclusions or pigments after firing,

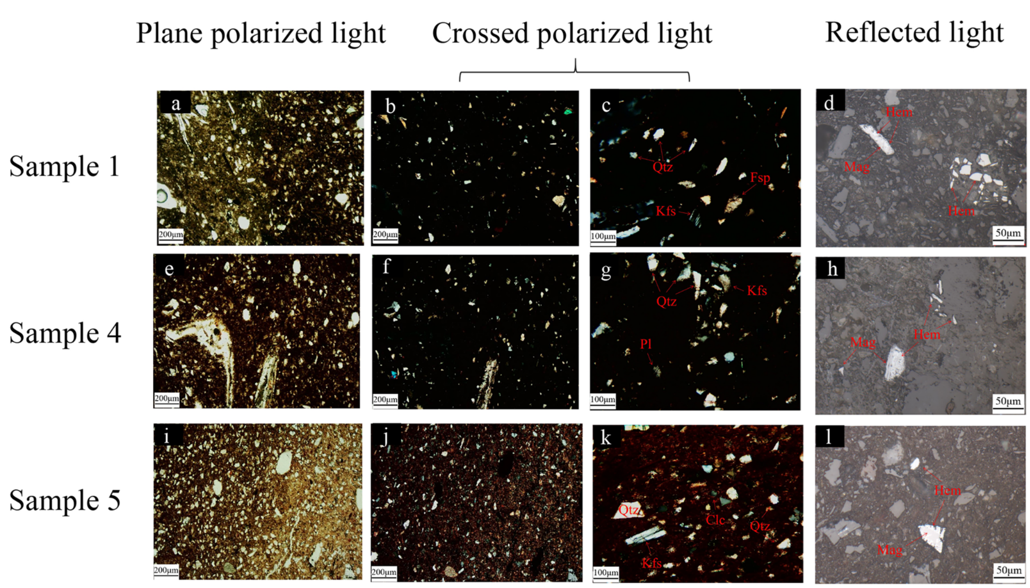

Fig. 4 Photomicrograph of a thin section from pottery samples. Photographs in the first and second columns of each sample are captured under the same field of view

Table 2 Main compounds and optical activity of samples

Sample No	Qz	Fsp	Ms	Cal	Chl	Bt	Hem	Mag	Optical activity
Sample 1	•	•	•	•		•	•	•	None
Sample 2	•	•	•	•		•	•	•	None
Sample 3	•	•	•	•		•	•	•	None
Sample 4	•	•	•	•			•	•	None
Sample 5	•	•	•	•	•	•	•	•	Very Low

Qz: quartz; Fsp: feldspar; Ms: muscovite; Cal: calcite; Chl: chlorite; Bt: biotite; Hem: hematite; Mag: magnetite; • -present

Table 3 Mineralogical composition of the shards according to XRD analysis

Sample No	Qz	Pl	Mcc	Ms	Mnt	Kln	Cal
Sample 1	50	22	10	18	–	–	–
Sample 2	51	17	14	18	–	–	–
Sample 3	53	15	10	22	–	–	–
Sample 4	56	25	15	4	–	–	–
Sample 5	48	11	7	13	13	5	3

Pl: plagioclase; Mcc: microcline; Mnt: montmorillonite; Kln: kaolinite

as it appeared on or near the pottery surface. Sample 5 shared the main mineral components with Samples 1–3, with additional minor minerals such as chlorite.

All samples showed oblong pores, potentially generated after burning straw or other plants added as temper in the clay paste (Additional file 1: Fig. S2). Clay and silt content were lower in Samples 1–4 and higher in Sample 5, suggesting raw materials may have been derived from alluvial soils or subjected to repeated panning [16].

The color of clay paste, indicative of firing atmosphere, ranged from yellowish brown to brownish black, suggesting a valence of Fe at + 3 and thus oxidation during pottery firing [17]. The proportion of hematite to magnetite in the pottery provided additional evidence of oxidation conditions during the firing process, with the hematite content surpassing that of magnetite [16].

Samples exhibited a sandwich structure with a darker core and lighter surface, indicating incomplete oxidation inside the body [18]. Organic materials were not fully burned out, leaving carbon residue in the middle of the pottery. Sample 4, lighter in color, suggested nearly complete combustion of organic matter.

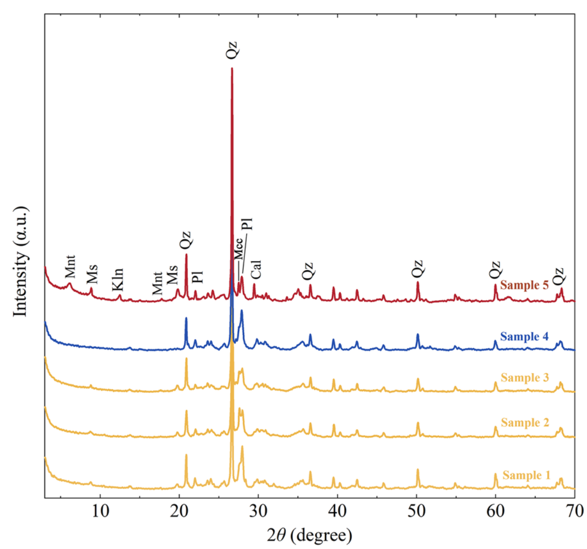

Fig. 5 XRD patterns of pottery samples

X-ray diffraction

XRD analysis identified the primary mineral phases as quartz, plagioclase, microcline, and muscovite across all samples, as detailed in Table 3 and Fig. 5. Sample 5 exclusively exhibited the presence of kaolinite, montmorillonite, and calcite. Quantitative results were derived from peak areas. However, it is important to note that these results may be influenced by factors such as microstructure and mass absorption, thus requiring careful interpretation [19]. Nonetheless, they provide a valuable reference point.

Infrared spectroscopy

FT-IR spectra, previously published in Chinese [15], were further analyzed using second derivative (Fig. 6). Peak assignments were made based on relevant literature [20] and the RRUFF database, and mineral abundance

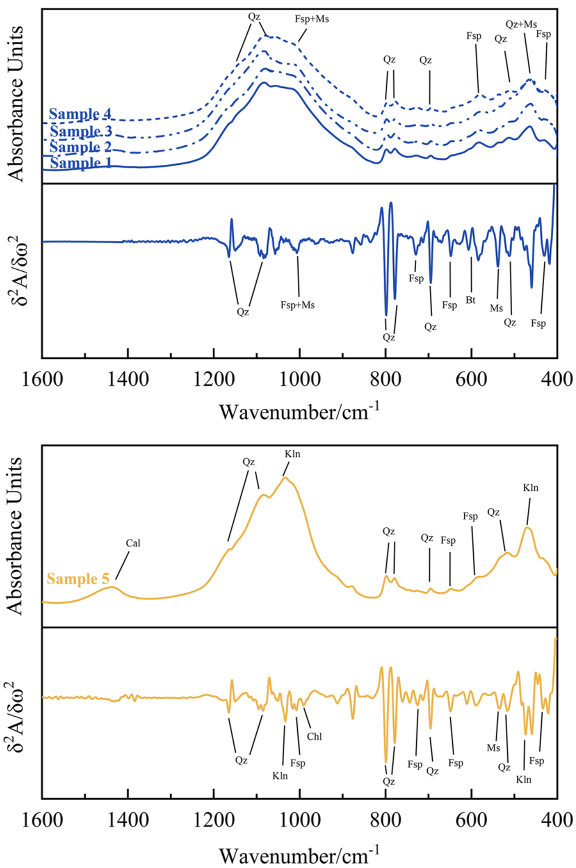

Fig. 6 FT-IR patterns of pottery samples [15] and their second derivative

was estimated based on the ratio of peak intensity to the intensity of the quartz absorption peak (1080 cm^{-1}). Results are presented in Table 4. All shards were similar and could be divided into two groups. As shown in Table 4, quartz, feldspar, and muscovite were present in all infrared spectra. Sample 5, however, featured additional minerals such as chlorite, calcite, and kaolinite.

X-ray fluorescence

Elemental analysis exhibited consistent distribution of major elements, classifying the clay as general fusible clay [5] based on its composition—SiO_2 (65.80–67.09 wt%), Al_2O_3 (14.44–16.12 wt%), and total flux content (17.21–20.50 wt%)—with low elemental Ca content (less than 6%) suggesting the use of non-calcareous clay [21] (Fig. 7; Additional file 1: Table S1).

The main differences in the distribution of elemental content were observed in the K content of Sample 3 and the elemental Mg content of Sample 5. The high content of P and K in Sample 3 could be attributed to plant inclusions at the sampling location, as biomass materials are rich in these elements. The overall elemental compositions in all five samples supported the speculation of consistent soil sources.

Discussion

Mineralogical results

The combination of three analytical methods—optical microscopy in polarized light, XRD, and FT-IR—yielded comprehensive results, as these methods complemented each other. XRD effectively identified crystalline minerals, while FT-IR was effective for analyzing both crystalline and non-crystalline materials [20].

All samples exhibited consistency in their main components, including quartz, plagioclase, microcline, muscovite, hematite, and magnetite. Further categorization based on minor components revealed that Sample 4 shared similarities with Samples 1, 2, and 3, with the absence of biotite being the distinguishing factor. In contrast, Group 2 comprised only Sample 5, characterized by the presence of chlorite, montmorillonite, calcite, and kaolinite. This grouping aligns with the classification based on pottery texture.

Firing techniques

Insights into firing techniques were gleaned from the formation and disappearance of minerals at specific temperature ranges. Phase transitions, indicative of firing temperature, were evident in the mineral composition. For example, feldspars typically melt around 1100 °C [22, 23], while orthoclase decomposes at 1050 °C [20]. The decomposition temperature of calcite ranges from 650 to 750 °C, with complete decomposition occurring at 800–850 °C [24–26]. Chlorite exists below 700 °C [27], and the decomposition of kaolinite and the formation of metakaolinite occur in the temperature range of 500–650 °C [28–30].

Table 4 Mineralogical composition of the shards according to the infrared analysis

Sample No	Qz	Mcc	Ms	Kln	Cal	Hem	Chl
Sample 1, 2, 3 and 4	***	*	*			tr	
Sample 5	***	*	0*	*	tr	tr	tr

Number of asterisks indicates relative abundance

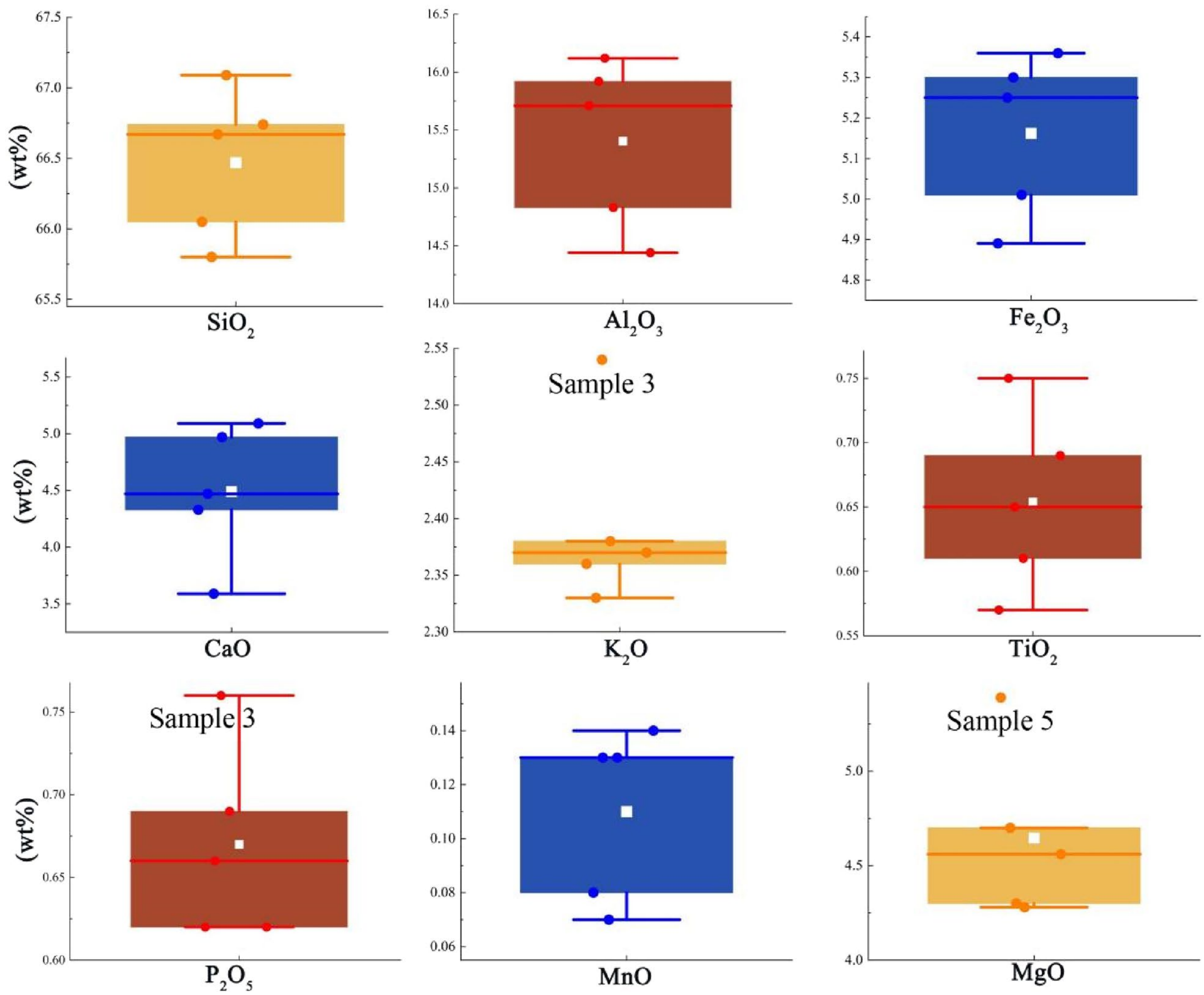

Fig. 7 XRF patterns of pottery samples

The observed variation in minor components among samples was attributed to differences in firing temperature. Samples 1–4 exhibited firing temperatures between 800 °C and 1100 °C, while Sample 5's firing temperature was below 650 °C, a conclusion corroborated by polarizing microscope analysis. Sample 5 displayed low optical activity, while samples 1–4 exhibited no optical activity in the matrix, and quartz exhibited less angular structure, indicating firing temperatures exceeding 900 °C [31]. The differences in minor components, including the absence of chlorite, kaolinite, montmorillonite, and calcite, were fully explained by variations in firing temperature.

Origin of polychrome pottery towers

Despite minor differences in minor mineral components and elemental contents, likely due to variations in firing temperature and uneven plant inclusions, respectively, all samples exhibited similarities in bulk composition, element content, plant inclusions, and firing atmosphere. The negligible differences in raw materials among the five samples suggest a consistent origin for pottery in the Daqu burial site.

The coarse potteries (Sample 5), characterized by low value, vulnerability, weight, and ease of production, were improbable products of inter-regional trade [32]. Consequently, the fine pottery towers (Samples 1–4) were likely crafted locally. This inference aligns with the notion proposed by Tite et al. [33] that large and heavy pottery types frequently found at a site are typically produced nearby. Notably, three pottery building samples (Sample 1–3) from different tombs and periods displayed nearly identical raw materials and techniques. Given the similarities in architectural structures and consistency in decorative details [15], it is reasonable to suggest that the polychrome towers were crafted following the same tradition [34], perhaps originated from the same workshop. Their high consistence in quality demonstrates the advanced techniques of ancient workers.

These findings contribute to the understanding of the late Han Dynasty. Variations in the quality and volume of potteries in the Daqu burial site may be linked to their different roles in the funeral system. Local producers likely designed and offered various Mingqi potteries for distinct purposes, emphasizing the importance of comparing the usage and quality of different potteries in other districts to explore customs during the late Eastern Han Dynasty and the interconnectedness between the central and northeastern regions of ancient China.

Conclusions

This study investigated materials and techniques employed for pottery in Han Dynasty at the Daqu burial site, marking the first use of scientific technologies on ancient Beijing potteries. Mineralogical and geochemical analyses revealed similarities in main components, elemental composition, plant inclusions, and firing atmosphere across all samples. Minor differences, particularly in minor minerals, were attributed to variations in firing temperature.

Archaeological information of pottery materials and firing techniques were obtained through OM, XRD, FT-IR, and XRF analyses. The results indicate that all pottery in the Daqu burial site utilized similar raw materials and techniques, and delicate polychrome pottery towers from different tombs likely originated from the same local workshop. Further studies on the economic and social conditions in the Beijing region during the Han Dynasty can build upon these results.

Supplementary Information

The online version contains supplementary material available at https://doi.org/10.1186/s40494-024-01245-x.

Additional file 1: Figure S1. Photomicrograph of thin section for Samples 2 and Sample 3; **Figure S2.** Microscopic images of pottery samples showing pores generated from burned plant fiber; **Table S1.** XRF test results of the chemical compositions of experimental samples.

Acknowledgements

Acknowledgments are attributed to Prof. Siran Liu, Institute for Cultural Heritage and History of Science & Technology, University of Science and Technology for his important suggestions during paper preparation and Fengdan Hu, China Academy of Cultural Heritage for her help in XRF and XRD analysis. We thank Dr. Ying Ma and Mr. Wenhua Zhao for their assistance in investigation and data acquisition.

Author contributions

Conceptualization, ZH and HG; Data curation, JW; Funding acquisition, NL and HG; Investigation, JW; Methodology, JW and IHG; Project administration, XH; Resources, NL; Supervision, XH; Validation, XH; Writing–original draft, JW and ZH; Writing–review & editing, XH.

Funding

This research was funded by the National Key R&D Program of China (Grant number 2023YFF0905903), the Fundamental Research Funds for the Central Universities (Grant number FRF-IDRY-22-009), and Technology analysis of polychrome pottery towers unearthed in Daqu burial site, Beijing Municipal Bureau of Cultural Relics.

Availability of data and materials

Data is contained within the article or supplementary material.

Declarations

Competing interests

The authors declare no conflict of interest.

Received: 28 January 2024 Accepted: 13 April 2024
Published online: 18 April 2024

References

1. Juan H. A Study on the Tombs of Beijing area through the Late Eastern Han Dynasty to the Western Jin Dynasty [Master's thesis]: Jilin University; 2018.
2. Go I, Wen J, He X, Liu N, Guo H. A multi-analytical approach to identify ancient pigments used in pottery towers excavated from the Han Dynasty tombs. Heritage Sci. 2023;11(1):227.
3. Lewis CJ. Pottery towers of Han dynasty China. New York: New York University; 1999.
4. Li S. Han dynasty architectural burial objects. J Nat Museum China. 2012;09:101–21.
5. Xueying Z. Exploration on the source of the constructive burial objects in Han Dynasty. Cultur Relics Central China. 2003;03:54–62.
6. Guo Q. The Mingqi pottery buildings of Han Dynasty China, 206 BC-AD 220. Eastbourne, Britain: Sussex Academic Press; 2010.
7. Chen Z. On the Economic Historical Materials of Han Dynasty: People's Publishing House Of Shaanxi; 1980. 171–2 p.
8. Kurosawa M, Semmoto M, Shibata T. Mineralogical characterization of early bronze age pottery from the svilengrad-brantiite site, Southeastern Bulgaria. Minerals. 2022;12(1):79.
9. Borgers B, Ionescu C, Willems S, Barbu-Tudoran L, Bernroider M, Clotuche R. Continuity and diversity of Roman pottery production at Famars (northern France) in the 2nd-4th centuries AD: insights from the pottery waste. Archaeol Anthropol Sci. 2020;12(9):1–27.
10. Vlase D, Vlase T, Bunoiu M, Sfirloaga P, Ursut AG, Vlase G. Characteristics of late Neolithic pottery of the Zau culture: analysis of pottery samples from Iernut-Site II (Mures County, Romania). J Therm Anal Calorim. 2022;147(9):5351–63.
11. Oudbashi O, Naseri R, Cultrone G, Egartner I, Arizzi A. The pottery production from the Deh Dumen Bronze Age graveyard (South-Western Iran): a chemical, mineralogical and physical study. Heritage Sci. 2021;9(1):1–8.
12. Germinario C, De Bonis A, Barattolo F, Cicala L, Franciosi L, Izzo F, et al. Ceramic building materials from the ancient Témesa (Calabria region, Italy): Raw materials procurement, mix-design and firing processes from the Hellenistic to Roman period. J Archaeol Sci Rep. 2022;41: 103253.
13. Jibing G, Jiangwei L. Samples analysis of painted Taocanglou in Han Dynasty. Cult Relics Central China. 2015;05:110–5.
14. Xin L. Study of polychrome potteries excavated from Han Dynasty tombs at Macun and Baizhuang in Jiaozuo. Sci Conserv Archaeol. 2021;33(01):97–102.
15. Wen J, Liu N, He X, Go I, Guo H. Analysis of the firing and molding techniques of painted pottery towers excavated from the Daqu Tombs in Beijing (in Chinese with English abstract). Res Conser Cave Temples Earthen Sites. 2023;2(01):43–56.
16. Schiavon N, Soria V, Arruda AM, Beltrame M, Mirao J. "Losanga" decorated imitations of italic late republican black gloss tableware from

South-Western Iberia: a multi-analytical/microchemical characterization. Microchem J. 2016;124:712–8.
17. Issi A, Raskovska A, Kara A, Grupce O, Minceva-Sukarova B, Okyar F. Scanning electron microscopy and micro-Raman spectroscopy of slip layers of Hellenistic ceramic wares from Dorylaion/Turkey. Ceram Int. 2011;37(6):1879–87.
18. Shoval S. The firing temperature of a Persian-period pottery kiln at Tel Michal, Israel, estimated from the composition of its pottery. J Therm Anal Calorim. 1994;42(1):175–85.
19. Ouhadi VR, Yong RN. Impact of clay microstructure and mass absorption coefficient on the quantitative mineral identification by XRD analysis. Appl Clay Sci. 2003;23(1–4):141–8.
20. De Benedetto GE, Laviano R, Sabbatini L, Zambonin PG. Infrared spectroscopy in the mineralogical characterization of ancient pottery. J Cult Herit. 2002;3(3):177–86.
21. Coria-Noguera JC, Badreshany KP, Sanz MC. Archaeometric characterization of pottery from the Iron Age hillfort of Pintia (Valladolid, Spain). J Archaeol Sci Rep. 2022;41: 103313.
22. Quinn PS. The Interpretation of Archaeological Pottery and Related Artefacts in Thin Section. Ceramic Petrography. Oxford, Britain: Archaeopress 2013. p. 42–53.
23. Papadopoulou DN, Lalia-Kantouri M, Kantiranis N, Stratis JA. Thermal and mineralogical contribution to the ancient ceramics and natural clays characterization. J Therm Anal Calorim. 2006;84(1):39–45.
24. Maggetti M, Neururer C, Ramseyer D. Temperature evolution inside a pot during experimental surface (bonfire) firing. Appl Clay Sci. 2011;53(3):500–8.
25. Fabbri B, Gualtieri S, Shoval S. The presence of calcite in archeological ceramics. J Eur Ceram Soc. 2014;34(7):1899–911.
26. Maggetti M. Composition of roman pottery from Lousonna (Switzerland). Scientific studies in ancient ceramics. 1981. 19: p. 33–49.
27. Shoval S. Using FT-IR spectroscopy for study of calcareous ancient ceramics. Opt Mater. 2003;24(1):117–22.
28. Ravisankar R, Annamalai GR, Naseerutheen A, Chandrasekaran A, Prasad MVR, Satpathy KK, et al. Analytical characterization of recently excavated megalithic sarcophagi potsherds in Veeranam village, Tiruvannamalai dist., Tamilnadu, India. Spectrochimica Acta Part Mol Biomol Spect. 2013;115:845–53.
29. Ravisankar R, Naseerutheen A, Rajalakshmi A, Raja Annamalai G, Chandrasekaran A. Application of thermogravimetry–differential thermal analysis (TG–DTA) technique to study the ancient potteries from Vellore dist, Tamilnadu, India. Spectrochim Acta Part A Mol Biomol Spectrosc. 2014;129:201–8.
30. Peters T. Mineralogical changes during firing of calcium-rich brick clays. 1978.
31. Allepuz ET. Colour transformation and textural change in biotite: some remarks for the interpretation of firing technology in greyware pottery thin-sections. Minerals. 2021;11(4):428.
32. Greene K. The archaeology of the Roman economy. Berkeley: Univ of California Press; 1986.
33. Tite MS. Pottery production, distribution, and consumption: the contribution of the physical sciences. J Archaeol Method Theory. 1999;6(3):181–233.
34. Grifa C, Germinario C, De Bonis A, Cavassa L, Izzo F, Mercurio M, et al. A pottery workshop in Pompeii unveils new insights on the Roman ceramics crafting tradition and raw materials trade. J Archaeol Sci. 2021;126: 105305.

Publisher's Note